A Potential Field Approach to Dexterous Tactile Exploration of Unknown Objects

Alexander Bierbaum, Matthias Rambow, Tamim Asfour and Rüdiger Dillmann
Institute of Computer Science and Engineering (CSE)
University of Karlsruhe (TH)
Karlsruhe, Germany
{bierbaum,rambow,asfour,dillmann}@ira.uka.de

***Abstract*—Haptic exploration of unknown objects is of great importance for acquiring multi-modal object representations, which enable a humanoid robot to autonomously execute grasping and manipulation tasks. In this paper we present a tactile exploration strategy to guide an anthropomorphic five-finger hand along the surface of previously unknown objects and build a 3D object representation based on acquired tactile point clouds. The proposed strategy makes use of the dynamic potential field approach suggested in the context of mobile robot navigation. To demonstrate the capabilities of this strategy, we conduct experiments in a detailed physics simulation using a model of the five-finger hand. Exploration results of several test objects are given.**

I. Introduction

Active touch exploration enables human not only to perceive local physical object features as texture or rigidity but also to sense the exact shape of an object.

The role of exploration is of utmost importance for an intelligent agent in order to learn control strategies. One can distinguish between direct and indirect exploration schemes, where undirected schemes are based on randomness and directed schemes try to optimize the gain in knowledge following each exploration step. A lot of such exploration techniques were developed in the context of mobile robot navigation, where the purposes are mapping and navigating in unknown environments while avoiding obstacles, see e.g. [1]. In the context of tactile exploration a task is to increase information of the shape of an object or more general, a part of the environment. For robots and especially for humanoid robots, tactile perception is supplemental to the information given by visual perception and may directly be exploited to augment and stabilize a spatial representation of real world objects. In the following we will give an overview on the state of the art achieved in robot tactile exploration and related approaches.

A directed tactile exploration strategy on the basis of a polyhedral object model was presented in [2]. The strategy is based on primitive movement of a single sensor, where a move becomes selected when it reduces the number of model interpretations from the exploration data by a maximum amount. The approach depends on sensing polyhedral features such as edges and is therefore not suitable for smooth objects. In [3] different single finger exploration strategies are presented, where a sensor movement direction is determined which provides a balance between the maximum decrease in global model uncertainty and the traveling distance of the sensor. Then the target region for starting the exploration process is approached using this direction vector. The results of a tactile exploration experiment for shape recovery using a robot finger are described in [4]. Here, a surface tracking strategy maintaining constant contact force was applied. The direction of motion on the tangent plane of contact was determined as the direction of maximum deviation between contact normal measurement and a second order local surface approximation. In the research area of dexterous manipulation of unknown objects various approaches for grasping under uncertainty have been presented. Especially to mention is the grasp controller for a multifingered robot hand using contact force feedback in [5]. Further, approaches for dexterous grasp control using probabilistic modelling have been presented in [6] and [7].

All previous approaches in robot tactile exploration for surface reconstruction did not cover the problem of controlling multifinger robot hands during the exploration process. Also, real world constraints such as manipulator limits or robustness over measurement errors have not been considered. In this paper we present first results on the application of a dynamic potential field control technique for guiding a multifinger robot hand across the surface of an unknown object, which is novel in the research area of dexterous manipulation. Artificial potential fields for robot control were introduced in [8]. Here, the manipulator follows the streamlines of a field where the target position is modelled by an attractive potential and obstacles are modelled as repulsive potentials. Potential fields may be constructed using superposition, therefore the method is cheap in computation compared to planning methods using explicit search. On the other hand, the method is vulnerable towards local minima which is a major caveat opposed to complete planners, thus precautions must be taken. In [9], a method for potential field based exploration with mobile robots has been presented. Here the world is represented in a grid-based model, where each cell has a certainty value representing a state in terms of occupied, unexplored or free space. An activation window around the agent limits the set of cells considered during each control cycle to those cells within a

certain distance around the agent. From the certainty value of the cells within this activation window a potential field is constructed which guides the agent avoiding obstacles while being attracted from unexplored regions and thus maximizing knowledge gain.

In our approach we have transferred the idea of potential field based exploration to tactile exploration for surface recovery using an anthropomorphic robot hand. As we believe that robustness and applicability of a tactile exploration strategy enhancing object model knowledge depends significantly upon the deployed hardware configuration, we have evaluated our approach in the framework of a physical simulator, reflecting non-neglectable physical effects such as manipulator kinematics, joint constraints or contact friction. As in related approaches we initially limit our scope to exploration of static scenes, which means the objects are fixated during exploration and may not move during interaction, although we wish later to develop means of pose estimation and tracking for object in dynamic scenes.

This paper is organized as follows. In the next two sections a short introduction to the potential field technique is given and the relevant details of the robot model are described. In Section IV we present the structure of the exploration process for the robot hand. Further, we show our simulation scenario and exploration results in section V. Finally, we give a conclusion and an outlook on our future work in Section VI.

II. Potential field control

Artificial potential fields have originally been introduced for the purpose of on-line collision avoidance in the context of robot path planning [8]. In the original approach, real-time efficiency was emphasized over obtaining a complete planner. The basic idea is that the robot behaves like a particle influenced in motion by a force field. The field is generated by artificial potentials Φ_i, where obstacles are represented as repulsive potentials $\Phi_r(x) > 0$ and goal regions are represented as attractive potentials $\Phi_a(x) < 0$. The superposition property allows to combine potentials in an additive manner,

$$\Phi(x) = \sum_i \Phi_{r,i}(x) + \sum_j \Phi_{a,j}(x) \quad . \tag{1}$$

The force vector field or potential field F, which influences a *Robot Control Point* (RCP) at position x is defined as

$$F = -\nabla\Phi(x) \quad .$$

Thus, the direction of the force vector gives the direction of steepest descent towards the goal configuration inside the potential field. A major drawback of potential fields is the existence of local minima outside the goal configurations in which the imaginary force exerted on an RCP is zero. By applying certain potential functions it is possible to construct potential fields without spurious local minima [10]. Further, by adding, moving or removing potential sources over time the potential field may be reconfigured continuously, which leads to the notion of dynamic potential fields.

While path planning should deliver a trajectory to a specified target using the information of free and collision space, this may not be the case in an exploration task. Here it may be the goal to acquire information about free and collision space, as e.g. in a *Simultaneous Localization and Mapping* (SLAM)-Task. This type of problem may be handled using dynamic potential fields, where regions of interest are assigned to attractive potentials which are changed neutral after attendance by the exploring agent. This way the location of the closest minimum of the potential field is changed so that the agent is attracted to a new region of interest. Note, that obstacles may still be modelled by using repulsive potential sources and thus collision free traveling is possible during exploration.

The notion of mobile robot exploration may not be transferred immediately to the task of tactile exploration. In tactile exploration it is not desired to avoid contact between the manipulator and an unknown object but rather trying to establish it. Therefore, the goal of the exploration process is not to determine a collision-free path but to solve a contour following problem along the surface of an unkown object.

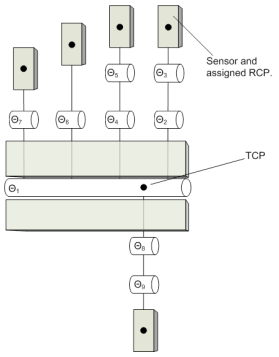

Fig. 1. Kinematics of the robot hand with joint axes, contact sensor locations (grey shaded) with assigned RCPs (black dots) and the TCP.

III. Robot hand kinematics, control and sensors

In our exploration approach we consider a setup comprising a 6-DoF manipulator arm with a five finger robot hand attached to its *Tool Center Point* (TCP). The manipulator arm was modelled according to the Mitsubishi RM-501 five axis small-scale industrial manipulator, which is currently used as research platform for dexterous haptic exploration in our lab. The model was augmented with a sixth DoF before the TCP to provide a larger configuration space. In our exploration control scheme we apply controller outputs to a set of five RCPs, located at the fingertips of the robot hand and to the TCP of the manipulator. The kinematic model of the robot hand is shown in Fig. 1. The hand model provides nine degrees of freedom and is modelled according to the FRH-4 Hand presented in [11]. During haptic exploration we are interested in controlling the velocity vectors of the RCP's, which is a different task compared to trajectory control. In trajectory control the end-effector is commanded to follow a desired trajectory with the motion control goal of asymptotic tracking. Yet, the given exploration task does not induce specific trajectories due to the uncertainty in the environment.

Therefore, we encode our task by means of a dynamic velocity field. Velocity field control was introduced in [12] for robot tasks such as contour following in robot surface inspection or painting tasks. In our approach we compute the velocity vector applied to an RCP directly from the dynamic potential field, which guides the exploration process. For evaluating our concept in a physics simulation environment it was not required to develop a solution to the multipoint end effector inverse kinematic problem. Instead we chose to take advantage of the physical model of the robot system and directly specify velocity vectors to the RCPs by using a virtual actuator which is commonly available in physics simulation frameworks. This way the joint angles are determined by solving the constrained rigid body system and a stable and consistent configuration of the robot hand is maintained. In general, this approach is known as *Virtual Model Control* (VMC), which is described in detail in [13]. In our case we specify joint constraints and joint friction for the robot model for achieving an appropriate force distribution over the joint serial paths, while we do not model a compliant behavior.

During exploration we control the velocity of the TCP with the VMC scheme, while we use a geometric solution of the inverse kinematics during the initialization phase of the system. In this phase the TCP is moved to a suitable initial configuration for starting the exploration process, which states a trajectory control problem.

For haptic exploration contact sensors are required which we have modelled in our physics simulation. Of course the simulation environment itself may be regarded as omniscient and therefore it is possible to query all contact locations and force vectors during the interaction of modelled physical bodies. We restricted contact sensing to dedicated sensor areas which cover the fingertips and the palm of the robot hand, see also Fig. 1. Further, we did not consider the contact force vector but only the contact location on the sensor area to provide a more realistic sensor model. This complies with current tactile sensor technology which in general can not provide both types of information. It is also possible to model more specific sensor characteristics such as a certain resolution in contact location or contact force tresholding, which we did not yet consider in our experiments.

As physics simulator we use a simulation tool based on the *Inventor Physics Modeling API* (IPSA) which was introduced in [14]. This simulator allows easy specification of complex dynamic and kinematic models using a physics extension of the *Open Inventor 3D Visualization Toolkit*[1].

IV. Dexterous tactile exploration

The goal of our work is the recovery of an unknown objects 3D shape by actively touching the object with an anthropomorphic robot hand and continuously moving the fingers to new locations on the surface. As prerequisite a rough initial estimate about the objects position, orientation and dimension is required. In simulation we introduce this information to the system, while this information is provided by a stereo camera system in the real application.

A. Potential field initalisation

During exploration we hold information about the environment in different structures. From an initial estimation, a global set of attractive potential sources $P_a = \{\vec{p}_i\}$ is constructed as a uniform grid around the estimated location of the exploration object, where $\vec{p}_i = (x, y, z)^T$ denote the source locations. We call the region occupied by this P_a the exploration space. A global set of repulsive potential sources $P_r = \{\vec{p}_i\}$ is initialized to $\emptyset$. The state of P_a and P_r will change during exploration, when the sensors detect contacts.

B. Object model generation and dynamic potential field

We update the potential sources according to the contact informations we obtain from the finger and the palm sensors. Whenever a sensor detects a contact inside the exploration space, we add a repulsive potential source $\vec{p}_c$ to P_r at the contact position.

An attractive potential source $\vec{p} \in P_a$ is deleted, when the distance $d = \|\vec{p} - \vec{p}_f\|$ to a fingers position is below a threshold d_{min}. We choose d_{min} to be somewhat larger than the fingertip dimension. Therefore, the deletion of an element in P_a implies that its immediate neighborhood has been explored.

Applying this scheme we obtain an object representation in P_r in terms of contact locations and automatically adjust the regions of interest represented by P_a.

From the two sets P_a and P_r we compute the potential field and the local gradient for each RPC of the robot hand. Therefore, we create a grid window of dimension N^3 for each RCP which is centered at its position $\vec{p}_{rcp} = (x, y, z)^T$ and calculate the potential at each grid point $\vec{p}_g$ according to eq. 1, where $\Phi_a = c_a \cdot \Psi_a(\vec{p}_{rcp})$ and $\Phi_r = c_r \cdot \Psi_r(\vec{p}_{rcp})$.

For $\Psi_a(\vec{p})$ and $\Psi_r(\vec{p})$ we apply a harmonic function as proposed in [10]. Using a harmonic function results in a monotone potential function which overall decreases the number of local minima during exploration.

To keep the potential field bounded we alter only the source distribution and preserve the field energy, which is expressed by

$$c_a = \frac{C_a}{|P_a|} \quad , c_r = \frac{-C_r}{|P_r|} \quad .$$

Further we maintain a certain balance between attractive and repelling sources by defining C_r as

$$C_r = k_P C_a, 0 < k_P < 1.$$

For computational reasons we perform a clustering of P_r in Euclidean space.

C. Velocity generation

Let Φ denote the potential grid window surrounding an RCP. Given this potential grid window we are now able to calculate the gradient vector for each RCP from which we directly obtain an imaginary velocity vector $\vec{v}$

[1] http://oss.sgi.com/projects/inventor/

$$\vec{v} = -k_v \nabla \Phi, \tag{2}$$

where k_v scales the velocity to our needs.

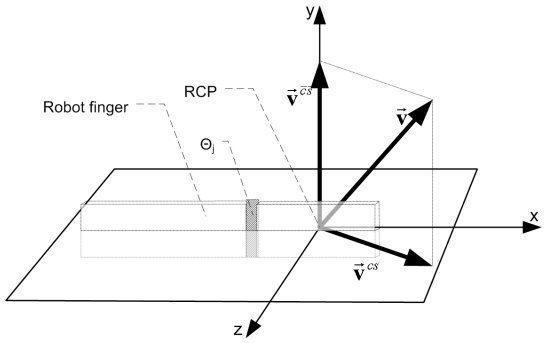

Fig. 2. RCP velocity computation during non-contact state.

As the RCPs' movements are constrained to their respective configuration space, each velocity vector $\vec{v}_i$ is decomposed into a portion $\vec{v}^{cs}$ situated in the plane containing the projection of the fingers configuration space onto the workspace and its orthogonal component $\vec{v}^{\overline{cs}}$. This decomposition is depicted in Fig. 2. The decomposed vector components are used to control the velocity of the TCP as

$$\vec{v}_{tcp} = [V_{cs}|V_{\overline{cs}}]\,\vec{k_c} \quad ,$$

where

$$V_{cs} = \left[\vec{v}_1^{cs} \cdots \vec{v}_{|RCP|}^{cs}\right] \quad , V_{\overline{cs}} = \left[\vec{v}_1^{\overline{cs}} \cdots \vec{v}_{|RCP|}^{\overline{cs}}\right] \quad .$$

Here, the elements of $\vec{k_c} = [k_{cs}, k_{\overline{cs}}]^T$ control the contribution of an RCPs' velocity to the velocity applied to the TCP. E.g. we consider index, middle finger and thumb to provide a greater proportion in guidance to the TCP during exploration than pinky and ring finger.

D. Exploration states

Ideally we want the fingers to follow the object surface contour. So we distinguish between two exploration states for each finger: a non-contact and a contact state. We assign a single contact sensor to each RCP, as shown in Fig. 1. The palm sensors are only used to detect contacts and do not provide feedback to an RCP. In case of a multi-contact situation on a single sensor we only consider the first contact reported. Self-collision of the robot hand engaging contact sensors is not handled explicitly but is for most configurations inhibited by the joint constraints. While a sensor does not detect a contact the local velocity vector $\vec{v}$ is applied to the assigned RCP according to eq. 2. Otherwise, in case of contact we project $\vec{v}$ onto the plane P characterized by the normal vector of the contact point.

This is depicted in Fig. 3. The contact normal vector is estimated as follows. We create a set $P_r^s \subseteq P_r$, which contains all potential sources that are inside the sphere with radius s surrounding the actual contact at $\vec{p}_c$:

$$P_r^s = \{\vec{p}_r \in P_r : \|\vec{p}_r - \vec{p}_c\| < s\}.$$

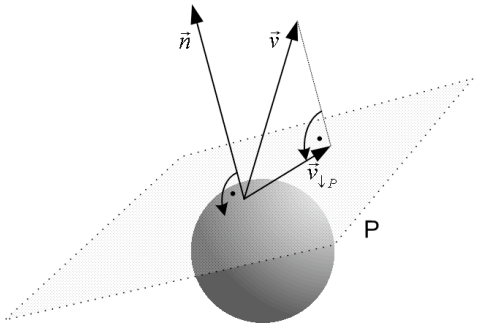

Fig. 3. RCP velocity computation in contact state. Here a contact of an RCP on a sphere is shown.

In case $|P_r^s| > 4$, we are able to compute the convex hull of P_r^s that provides a set $CH = \{\vec{p}_{r_1} \times \vec{p}_{r_2} \times \vec{p}_{r_3} : \vec{p}_{r_i} \in P_r\}$ of triangles that constitutes the convex hull. In the event of $\vec{p}_c$ being part of the convex hull we can now estimate its normal vector $\vec{n}_{est}$ as the mean vector of all triangles in CH containing $\vec{p}_c$ (see Fig. 4). If $\vec{p}_c$ is not part of the convex hull we discard this policy and use the primary velocity vector. Alternatively, we could search for the closest $\vec{p}_r \in P_r^s$ contained by the convex hull and use this vector as initial value for the normal estimation as well, but in this case $\vec{p}_c$ is likely to be near a non convex border of the exploration object. Using this scheme the RPC follows the estimated object surface contour in direction of the potential fields gradient during contact.

E. Reconfiguration policy

Although we may avoid local minima for a pointlike RCP using harmonic potentials, we can not eliminate deadlock situations of the complete robot system while interacting with the environment, i.e. the explored object. Since we do not model tactile sensors at phalanges distinct from the fingertips, deadlocks are likely to occur when a finger clings to the exploration object.

For identification of deadlocks we track the low pass filtered velocities of the TCP ν_{tcp} and the mean RCPs' velocity ν_{rcp}. We assume a deadlock situation once $\nu_{tcp} < \nu_{tcp}^{min}$ and $\nu_{rcp} < \nu_{rcp}^{min}$. Whenever a deadlock is identified we change from exploration to a reconfiguration state until ν_{tcp} exceeds an upper threshold ν_{tcp}^{max}. Similar we introduce a second threshold $\nu_{rcp,2}^{min}$. If $\nu_{rcp} < \nu_{rcp,2}^{min}$ a large configuration to the systems initial configuration is initiated. The values for ν_{tcp}^{min}, ν_{rcp}^{min}, $\nu_{rcp,2}^{min}$ and ν_{tcp}^{max} are determined empirically from experiments.

During reconfiguration all attractive potential sources become inverted to repulsive sources and the obtained new set of repulsive sources $P_r' = P_r \cup P_a$ is used for the RCPs' velocity generation. Furthermore, we directly generate a velocity vector for the TCP in the same way we do for the RCPs using P_r' and an additional attractive source $P_a' = \{\vec{p}_{tcp} - \vec{p}_{\overline{r}}\}$, where $\vec{p}_{tcp}$ denotes the TCP's position and $\vec{p}_{\overline{r}}$ the mean position of the attractive potential sources in P_a. This way the TCP position

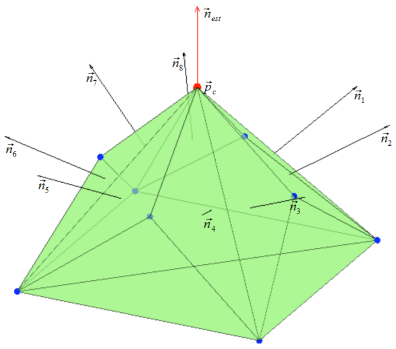

Fig. 4. Estimation of the local surface normal vector.

becomes adjusted towards a previously unexplored goal region during reconfiguration.

F. Palm reorientation

Up to now only translational velocities have been applied to RCPs, while rotational motion was forced indirectly via the joint constraints.

The robot arm model includes two DoF that allow to control the hands orientation in terms of pitch and roll. These allow allignment of the palm normal $\vec{n}$ to a preferred direction $\vec{m}$ that is calculated as $\vec{m} = \vec{p}_a^w - \vec{p}_{tcp}$, where $\vec{p}_a^w$ is the center of mass of all attractive potential sources $a(\vec{p}) \in P_a$ within a distance d_m of the current TCP position. We set d_m to be in the range of the length of a finger. The palm normal $\vec{n}$ is calculated as the mean of the normal vectors of the two palm faces around joint axis Θ_1. We realize the alignment by additional force-limited orientation control of the TCP. The control command is superimposed to the indirect constrained joint motion. The effect of this modification is that the robot hand will adjust its orientation towards the center of mass of all reachable attractive potential sources, which prevents the potential field control from turning the inner side of the hand away from the exploration scene.

G. Finger motion coupling

As we use an anthropomorphic hand model, it is desirable to avoid unnatural finger configurations. Otherwise, the individual RCP control might lead to a hand configuration in which fingers stick out of the hand. We achieve a natural, coupled motion of the finger joints by augmenting the joint velocity from constrained motion with the output of a force-limited joint angle controller. Therefore, we calculate the mean joint angle $\overline{\gamma}$ over all finger joint angles γ_j. The additional angular joint velocities ω_j of the finger joints Θ_j , $j \in A := \{2, ..., 9\} \subseteq \mathcal{N}$ are set to

$$\omega_j = sgn(e_j) \cdot \mathcal{F}(|e_j|) \cdot \omega_{max}$$

where the control error e_j is calculated using a joint coupling $k_j \in [0, 1]$

$$e_j = k_j(\overline{\gamma} - \gamma_j)/\gamma_{max} \quad .$$

We limit the maximum force F_{max} allowed to apply by the controller to

$$F_{max} = \mathcal{F}(|d(\gamma_j)|) \cdot F_0 \quad .$$

Here, $\mathcal{F}$ is a strictly monotone increasing function $[0, 1] \rightarrow [0, 1]$. The joint coupling k_j lets us choose to align some joints more or less to $\overline{\gamma}$ than others. For example the joints for the ring and the little finger are coupled fully with a factor $k_j = 1$ whereas the k_j of the middle finger, index and thumb joints are set to a lesser factor so they may move more flexible during exploration.

V. Simulation Results

We evaluated our potential field based haptic exploration approach with exemplar virtual scenes using a physics simulator. The virtual scenes were set up with different objects from which we automatically generated initial estimation parameters as described in section IV. With these parameters the exploration space was computed according to the cubical bounding box of the object. We chose three different objects, a sphere, a cylinder and a telephone receiver model as a more complex object. With the current implementation of our physics simulation the objects have to be nearly convex as otherwise the collision detection function can not properly detect contacts with non-convex objects engaged. For the sphere and cylinder objects we varied positions, orientation and size in the experiments. We limited the exploration duration to 2500 iteration steps of the physics simulation, with step time $T = 0.04s$. All control specific parameters and thresholds as described before were chosen constant and independent of the object explored for all experiments. The explored scene is static, i.e. the object explored is fixated so it may not be moved by the physical interaction during contact. In our experiments we placed the objects floating above the ground plane in the simulation, so the robot hand may also explore the bottom side of the object.

The exploration progress is shown in Fig. 5. The notions of close and distant object placement are meant relative to the configuration space of the robot hand. A distant placed object is more difficult to reach and to establish contact with all sides. As can be seen, the contact acquisition is continous, while traversal of unvisited exploration space decreases over time, because remaining attractive potentials are more and more situated inside the space occupied by the object. Also, objects placed in poses difficult to reach require a significant higher number in reconfigurations. The example reconfiguration progress plots in Fig. 5(b), 5(d), 5(f) show the progression of ν_{rcp} (blue) and ν_{tcp} (red). The horizontal lines indicate the threshold values ν_{tcp}^{min} (lower black line), ν_{rcp}^{min} (upper black line), ν_{tcp}^{max} (green), $\nu_{rcp,2}^{min}$ (blue). The vertical lines indicate reconfiguration start (turquoise) and end (black) respectively. We found that reconfiguration occured more often with decreasing reachability and increasing number of surface obstacles. With the telephone receiver model the robot hand happened more often to cling to the sharp edges of the structure, while this appeared less with the smooth

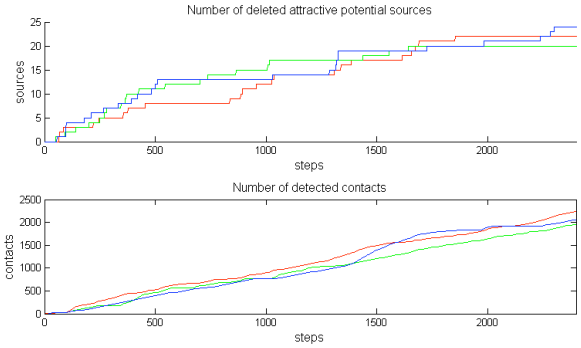

(a) Sphere of radius r. red: $r = 5cm$, close placement,$|P_a| = 64$, $N_r = 12$. green: $r = 3.2cm$, distant placement, $|P_a| = 27$, $N_r = 19$. blue: $r = 3.2cm$, close placement, $|P_a| = 27$, $N_r = 10$.

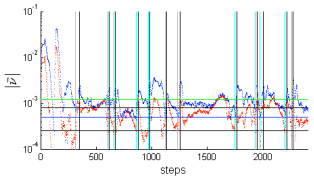

(b) Reconfiguration progress, sphere.

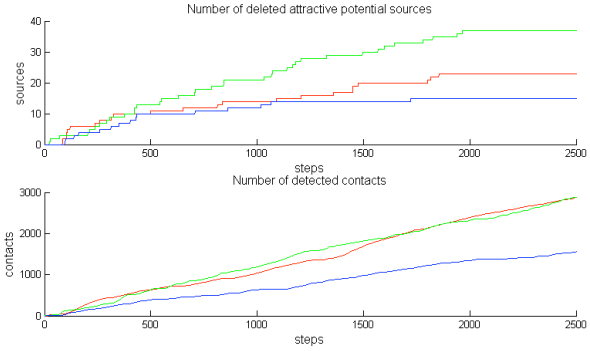

(c) Cylinder with radius r and length l. red: $r = 3cm$, $l = 9cm$, close placement, hor., $|P_a| = 36$, $N_r = 13$. green: $r = 3cm$, $l = 16cm$, close placement, hor., $|P_a| = 45$, $N_r = 25$. blue: $r = 4cm$, $l = 4cm$, close placement, vert., $|P_a| = 27$, $N_r = 22$.

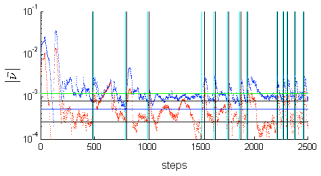

(d) Reconfiguration progress, cylinder.

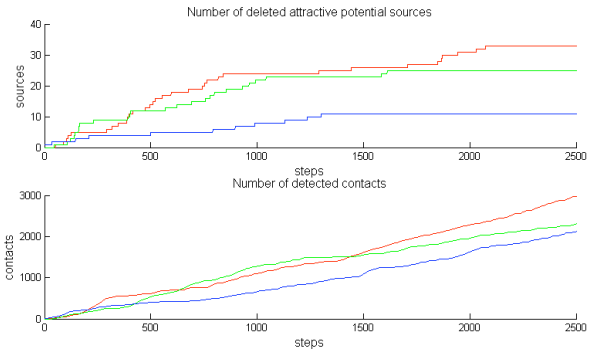

(e) Telephone receiver, $|P_a| = 54$. red: close placement, hor., $N_r = 19$. green: medium far placement, $45°$, $N_r = 25$. blue: distant placement, vert., $N_r = 35$.

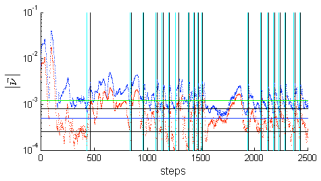

(f) Reconfiguration progress, telephone receiver.

Fig. 5. Exploration and reconfiguration progress plots for the test objects. N_r denotes the number of required reconfigurations.

surface of the sphere. Further, we observed that the proposed reconfiguration method managed to escape upcoming deadlock situations within one or several cycles in all scenes. So, the robot hand was guided around the object to establish contacts from all sides towards the object in the exploration space, if the object placement permitted the required hand configurations. The reconfiguration progress plots refer to the scene configuration represented by the first exploration progress plot (red) Fig. 5(a), 5(c), 5(e) for each object respectively.

Typical 3D contact point clouds resulting from haptic exploration are shown in Fig. 6. In fact, these plots show the final potential source arrangements after exploration, where the red dots indicate remainders in P_a and the blue dots are the set of P_r. The resulting haptic point clouds exhibit spots with less density especially at locations with sharp edges where the sensors often lose contact during the surface tracking phase. Naturally sparse are regions which are situated outside the fingers configuration space. Such regions are visible e.g in the

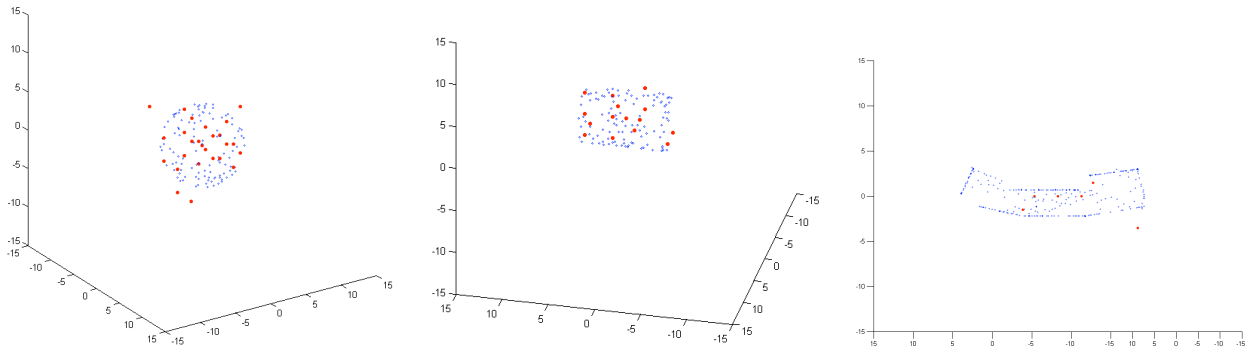

Fig. 6. Typical exploration results for the objects sphere, cylinder and phone after 2500 iterations. Red: P_a, Blue: P_r.

plot of the receiver at bottom left and right side.

VI. Conclusions

In this paper we presented a control scheme for tactile exploration of unknown objects with an anthropomorphic multifingered robot hand. Our approach is based on dynamic potential fields for motion guidance of the fingers. We added a potential field based reconfiguration strategy to eliminate deadlock situations which may occur due to local minima in the configuration space. Finally, we introduced finger joint motion coupling to provide natural trajectories of the robot fingers during exploration. We evaluated the complete control scheme in a detailed physics simulation of the robot system with test objects and presented the resulting 3D point clouds of explored objects and gave detailed report on the progress during exploration. Concluding, we are confident that the potential field based approach presented may be used for real world tactile exploration using an anthropomorphic robot hand as it appears robust enough to autonomously guide the robot hand over an unknown object providing tactile information to enhance the object model. We assume that the proposed scheme is transferable to different manipulator and robot hand kinematics by adapting parametrization, number of RCPs and RCP locations. We are planning to extend this approach to a method of potential field based grasping, which appears feasible from our observation of the hand and finger motion under potential field guidance. We regard the approach to be promising in our eyes and will combine this method with a vision based object exploration method to obtain a multimodal object model, which might enable us to extend the concept for dynamic scenes.

As a next step we will transfer the developed control scheme based on VMC and dynamic potential fields to our real world robot system equipped with five-finger hands [15] as soon as we have low level force and position control available with our robot hand.

Acknowledgement

The work described in this paper was conducted within the EU Cognitive Systems projects PACO-PLUS (FP6-027657) and GRASP (FP7-215821) funded by the European Commission.

References

[1] S. Thrun, "The role of exploration in learning control," in *Handbook for Intelligent Control: Neural, Fuzzy and Adaptive Approaches*, D.A. White and D.A. Sofge, Eds. Van Nostrand Reinhold, Florence, Kentucky 41022, 1992.

[2] K.S. Roberts, "Robot active touch exploration: constraints and strategies," in *Robotics and Automation, 1990. Proceedings., 1990 IEEE International Conference on*, 13-18 May 1990, pp. 980–985 vol.2.

[3] S. Caselli, C. Magnanini, F. Zanichelli, and E. Caraffi, "Efficient exploration and recognition of convex objects based on haptic perception," in *Robotics and Automation, 1996. Proceedings., 1996 IEEE International Conference on*, 22-28 April 1996, pp. 3508 – 3513 vol.4.

[4] N. Chen, R. Rink, and H. Zhang, "Local object shape from tactile sensing," in *Robotics and Automation, 1996. Proceedings., 1996 IEEE International Conference on*, 22-28 April 1996, vol. 4, pp. 3496–3501vol.4.

[5] J. Coelho and R. Grupen, "A control basis for learning multifingered grasps," *Journal of Robotic Systems*, vol. 14, no. 7, pp. 545–557, 1997.

[6] Kaijen Hsiao, L.P. Kaelbling, and T. Lozano-Perez, "Grasping pomdps," *Robotics and Automation, 2007 IEEE International Conference on*, pp. 4685–4692, 2007.

[7] R. Platt, "Learning grasp strategies composed of contact relative motions," in *IEEE-RAS International Conference on Humanoid Robots, Pittsburgh, PA*, Dec 2007.

[8] Oussama Khatib, "Real-time obstacle avoidance for manipulators and mobile robots," *The International Journal of Robotics Research*, vol. 5, no. 1, pp. 90–98, 1986.

[9] Edson Prestes e Silva, Paulo M. Engel, Marcelo Trevisan, and Marco A. P. Idiart, "Exploration method using harmonic functions," *Robotics and Autonomous Systems*, vol. 40, no. 1, pp. 25–42, July 2002.

[10] C.I. Connolly, J.B. Burns, and R. Weiss, "Path planning using laplace's equation," in *Robotics and Automation, 1990. Proceedings., 1990 IEEE International Conference on*, May 1990, vol. 3, pp. 2102–2106.

[11] I. Gaiser, S. Schulz, A. Kargov, H. Klosek, A. Bierbaum, C. Pylatiuk, R. Oberle, T. Werner, T. Asfour, G. Bretthauer, and R. Dillmann, "A new anthropomorphic robotic hand," in *IEEE-RAS International Conference on Humanoid Robots*, 2008.

[12] P.Y. Li and R. Horowitz, "Passive velocity field control of mechanical manipulators," in *Proc. IEEE International Conference on Robotics and Automation*, 1995, vol. 3, pp. 2764–2770 vol.3.

[13] J. Pratt, A. Torres, P. Dilworth, and G. Pratt, "Virtual actuator control," in *Proc. IEEE/RSJ International Conference on Intelligent Robots and Systems '96, IROS 96*, 1996, vol. 3, pp. 1219–1226 vol.3.

[14] A. Bierbaum, T. Asfour, and R. Dillmann, "Ipsa - inventor physics modeling api for dynamics simulation in manipulation," in *IROS - Workshop on Robot Simulation, 22. Sept. 2008, Nice, France*, 2008.

[15] T. Asfour, K. Regenstein, P. Azad, J. Schroder, A. Bierbaum, N. Vahrenkamp, and R. Dillmann, "Armar-iii: An integrated humanoid platform for sensory-motor control," in *Humanoid Robots, 2006 6th IEEE-RAS International Conference on*, Dec. 2006, pp. 169–175.